

# The role of the energy equation in the fragmentation of protostellar discs during stellar encounters

G. Lodato<sup>1</sup>, F. Meru<sup>1</sup>, C. J. Clarke<sup>1</sup> and W. K. M. Rice<sup>2</sup>

<sup>1</sup>*Institute of Astronomy, Madingley Road, Cambridge, CB3 0HA*

<sup>2</sup>*Scottish Universities Physics Alliance (SUPA), Institute for Astronomy, University of Edinburgh, Blackford Hill, Edinburgh EH9 3HJ*

5 July 2018

## ABSTRACT

In this paper, we use high-resolution smoothed particle hydrodynamics (SPH) simulations to investigate the response of a marginally stable self-gravitating protostellar disc to a close parabolic encounter with a companion discless star. Our main aim is to test whether close brown dwarfs or massive planets can form out of the fragmentation of such discs. We follow the thermal evolution of the disc by including the effects of heating due to compression and shocks and a simple prescription for cooling and find results that contrast with previous isothermal simulations. In the present case we find that fragmentation is inhibited by the interaction, due to the strong effect of tidal heating, which results in a strong stabilization of the disc. A similar behaviour was also previously observed in other simulations involving discs in binary systems. As in the case of isolated discs, it appears that the condition for fragmentation ultimately depends on the cooling rate.

**Key words:** accretion, accretion discs – gravitation – instabilities – stars: formation – planets: formation – brown dwarfs: formation

## 1 INTRODUCTION

Young stellar clusters are dynamic environments and encounters between cluster members can be quite common (see, for example, Figure 6 of Scally & Clarke 2001). Such encounters can have a significant effect on the structure and evolution of the gaseous discs that surround young stars (Bate et al. 2003). Some of these effects include a tidal truncation or disruption of the disc (Clarke & Pringle 1993; Hall et al. 1996), a burst of accretion activity onto the central star (Bonnell & Bastien 1992), or the triggering of a gravitational instability in the disc, which might then lead to disc fragmentation (Boffin et al. 1998; Watkins et al. 1998a,b). The latter possibility has been often invoked as a possible formation mechanism for low mass companions, such as brown dwarfs, or massive planets (for some recent reviews, see Whitworth et al. 2006; Goodwin et al. 2006). However, previous analyses of this process (Boffin et al. 1998; Watkins et al. 1998a,b) were limited by low resolution (which did not permit the proper resolution of the disc vertical structure) and by the replacement of the energy equation by a simple barotropic equation of state. All these analyses, in fact, assumed that the disc is isothermal, which might be a reasonable assumption at very large distances (the discs considered in these works are  $\approx 1000$  AU in size), but is certainly not adequate for smaller discs. Indeed, as clearly

stated in Whitworth et al. (2006) “it is important that such simulations be repeated, with a proper treatment of the energy equation... to check whether low-mass companions can form at closer periastra”. This is precisely the aim of the present paper.

The importance of cooling in determining the conditions under which a gravitationally unstable disc fragments has been clearly pointed out by Gammie (2001) initially from local shearing-box simulations and later confirmed in global disc simulations (Rice et al. 2003; Rice et al. 2005; Mejia et al. 2005). The general result is that fragmentation occurs only if the cooling timescale is smaller than a few times the dynamical timescale in the disc. This result can be understood in the following way. The linear stability of a rotating disc against axisymmetric gravitational perturbations is described by the well known Toomre parameter:

$$Q = \frac{c_s \kappa}{\pi G \Sigma}, \quad (1)$$

where  $c_s$  is the sound speed,  $\kappa$  is the epicyclic frequency (equal to the angular velocity  $\Omega$  in a Keplerian disc) and  $\Sigma$  is the disc surface density. The disc is unstable if  $Q < 1$ , so that local perturbations will grow on a timescale of the order of the dynamical timescale  $\Omega^{-1}$ . The linear stability then only depends on the disc temperature (through  $c_s$ ) and density  $\Sigma$ . However, the non-linear growth of the perturbations heats up the equilibrium state (through compression

and shocks), increasing the value of  $Q$  and hence stabilizing the disc, and preventing fragmentation, unless the heat produced by compression can be removed efficiently. Since the perturbation grows on the dynamical timescale, if we want to have fragmentation, we require that cooling acts on the same timescale.

Actually, an alternative way to destabilize the disc is to increase its surface density (rather than decreasing its temperature), which might result from the tidal interaction with a companion star. In a series of papers, Boffin et al. (1998) and Watkins et al. (1998a,b) have explored this possibility by simulating isothermal discs which are initially stable (with  $Q > 1$  throughout the disc) and are destabilized by stellar encounters. The process appears to be successful in that in general the disc can be effectively destabilized. However, in this case, the subsequent evolution of the system is essentially dictated by the isothermal condition: the perturbation will grow and produce substellar fragments. This is indeed what is observed in these simulations. However, it now becomes essential to determine whether - in the presence of heating and cooling - the strong, non-linear perturbation induced by the encounter would still be able to produce fragmentation, or whether, similarly to the case where the perturbation is induced more gently, through a slow cooling, fragmentation is instead inhibited.

Similar issues have also been considered, often including the effects of tidal heating and radiative cooling, in the context of planet formation in binary systems. However, the results up to now appear to be contradictory. Indeed, if on the one hand Nelson (2000) and Mayer et al. (2005) claim that the presence of a companion inhibits the formation of planets via fragmentation, Boss (2006), on the other hand, argues in favour of fragmentation.

In this paper, we present the results of a series of smoothed particle hydrodynamics (SPH) simulations of the encounter of a star surrounded by a gaseous disc with a disc-less companion. The gas disc is here allowed to heat up through compression and shocks and to cool down slowly, so that in isolation the disc does not fragment but attains a marginally stable, self-regulated state. We explore parameter space by varying the orbital properties of the stars, their mass ratio, and the mass ratio between the star and the disc. *None of our simulations resulted in fragmentation*, thus proving that also in this situation the main requirement to form substellar companions is that the cooling be fast. The disc is strongly perturbed and its density can be enhanced significantly, but the heat provided by compression strongly overcomes the density increase, resulting in a substantial stabilization of the disc.

The paper is organized as follows. In Section 2 we describe the SPH code that we use and the physical setup of our simulations. In Section 3 we describe the evolution of our reference run. In Section 4 we discuss the effects of changing the main parameters of the problem. In Section 5 we discuss our results and draw our conclusions.

## 2 NUMERICAL SETUP

### 2.1 The SPH code

Our three-dimensional numerical simulations are carried out using SPH, a Lagrangian hydrodynamic scheme (Benz 1990;

Monaghan 1992). The general implementation is very similar to Lodato & Rice (2004, 2005) and Rice et al. (2005). The gas disc is modelled with 250,000 SPH particles (500,000 in a run used as a convergence test) and the local fluid properties are computed by averaging over the neighbouring particles. The central star and the perturber are modelled as point masses onto which gas particles can accrete if they get closer than the accretion radius, taken to be equal to 0.5 code units for the central star and the high mass perturber (see below) and 0.25 code units for the small mass perturber.

The gas disc can heat up due to  $pdV$  work and artificial viscosity. The ratio of specific heats is  $\gamma = 5/3$ . Cooling is here implemented in a simplified way, i.e. by parameterizing the cooling rate in terms of a cooling timescale:

$$\left(\frac{du_i}{dt}\right)_{\text{cool}} = -\frac{u_i}{t_{\text{cool}}}, \quad (2)$$

where  $u_i$  is the internal energy of a particle and the cooling timescale  $t_{\text{cool}}$  is assumed to be proportional to the dynamical timescale,  $t_{\text{cool}} = \beta\Omega^{-1}$ . We know from previous work (Gammie 2001; Rice et al. 2005) that if  $\beta < 3 - 7$  (depending on the ratio of the specific heats) the disc is unstable to fragmentation. Our aim is to establish whether a disc that would not fragment in isolation can be driven to fragmentation as a result of a stellar encounter. We have therefore set  $\beta = 7.5$ , so that in isolation our disc is not expected to fragment.

### 2.2 Disc setup

The main physical properties of the disc at the beginning of the simulation are again similar to those of Lodato & Rice (2004) and Lodato & Rice (2005). The disc surface density  $\Sigma$  is initially proportional to  $R^{-1}$  (where  $R$  is the cylindrical radius), while the temperature is initially proportional to  $R^{-1/2}$ . Given our simplified form of the cooling function, the computations described here are essentially scale free and can be rescaled to different disc sizes and masses. For reference, we will assume that the unit mass (which is the mass of the central star) is  $1M_\odot$  and that the unit radius is  $1AU$ . In these units the disc extends from  $R_{\text{in}} = 0.25AU$  to  $R_{\text{out}} = 25AU$ . The normalization of the surface density is generally chosen such as to have a total disc mass of  $M_{\text{disc}} = 0.1M_\odot$  (in a couple of cases, however, we have also considered different disc masses, see below), while the temperature normalization is chosen so as to have a minimum value of  $Q = 2$ , which is attained at the outer edge of the disc. This is obtained by setting  $T \simeq 45$  K at the outer edge.

Initially, the disc is evolved in isolation for several outer dynamical timescales. The general features of this initial evolution is described in detail in Lodato & Rice (2004). The disc starts cooling down until the vertical scale-length  $H$  is reduced such that  $H/R \approx M_{\text{disc}}/M_\star = 0.1$ . At this point the disc becomes Toomre unstable and develops a spiral structure that heats up the disc and maintains it close to marginal stability, i.e. close to  $Q = 1$ , roughly independent of radius.

### 2.3 Adding the perturber

Once the disc has reached the quasi-steady, self-regulated state of marginal stability, we add the perturber star. This

Simulation	$M_{\text{disc}}/M_{\odot}$	No gas particles	$M_{\text{pert}}/M_{\odot}$	Orbit	Direction	eccentricity	$r_{\text{peri}}/\text{AU}$
S1	0.1	250,000	0.1	coplanar	prograde	1	17
S2	0.1	250,000	1.0	coplanar	prograde	1	17
S3	0.1	250,000	0.1	coplanar	retrograde	1	17
S4	0.1	250,000	0.1	'head on'	—	1	17
S5	0.1	250,000	0.1	coplanar	prograde	7	17
S6	0.05	250,000	0.1	coplanar	prograde	1	17
S7	0.2	250,000	0.1	coplanar	prograde	1	17
S8	0.1	250,000	0.1	coplanar	prograde	1	30
S9	0.1	250,000	0.1	coplanar	prograde	1	40
H1	0.1	500,000	0.1	coplanar	prograde	1	17

**Table 1.** Summary of the main physical properties of the simulations carried out.

is initially put at a distance of  $100\text{AU}$  from the primary star, and is placed in a parabolic orbit. At this distance, the sudden addition of the perturber does not cause any significant perturbation to the disc structure. We have performed a large number of simulations, by varying the orbital parameters, considering coplanar encounters (both prograde and retrograde with respect to the disc rotation) and 'head on' encounters, where the orbital plane of the secondary is perpendicular to the disc plane. We have also performed a simulation of a hyperbolic (coplanar) encounter. We have varied the disc mass, the perturber mass  $M_{\text{pert}}$  and the pericenter of the perturber orbit  $r_{\text{peri}}$  and we have also run simulations with different numerical resolutions. Table 1 summarizes the main physical setup of the various simulations that we have done.

## 2.4 Resolution issues

One important aspect that needs to be taken into account is whether our simulations have enough resolution to resolve the fragments, if fragmentation occurs. As shown by Bate & Burkert (1997), SPH correctly reproduces fragmentation if the Jeans mass is larger than the minimum resolvable mass, defined as:

$$M_{\text{min}} = 2N_{\text{neigh}}m_i = 2M_{\text{tot}} \left( \frac{N_{\text{neigh}}}{N_{\text{tot}}} \right), \quad (3)$$

where  $m_i$  is the mass of a single SPH particle,  $M_{\text{tot}}$  ( $= M_{\text{disc}}$  in this case) is the total mass of the gas being simulated,  $N_{\text{tot}}$  is the total number of SPH particles used, and  $N_{\text{neigh}}$  is the number of SPH neighbours (which is always kept close to 50).

To estimate the expected Jeans mass  $M_J$ , we use the fact that the most unstable wavelength to gravitational instability is of the order of the disc thickness  $H$ . We then have  $M_J \approx \Sigma H^2 \approx M_{\text{disc}}(H/R)^2$ , from which we get:

$$\frac{M_J}{M_{\text{min}}} \approx \frac{1}{2} \left( \frac{H}{R} \right)^2 \frac{N_{\text{tot}}}{N_{\text{neigh}}} \approx \frac{1}{2} \left( \frac{M_{\text{disc}}}{M_{\star}} \right)^2 \frac{N_{\text{tot}}}{N_{\text{neigh}}}. \quad (4)$$

For most of our simulations, we use 250,000 particles, which would then lead to  $M_J \approx 25M_{\text{min}}$ . We thus have more than enough resolution to properly address the issue of fragmentation. However, to be sure, we have also performed a convergence test of our results, by running a simulation with twice as many particles. The results of this convergence test are described below in Section 4.

The second aspect related to resolution is that we require artificial viscosity to play a role only when modeling shocks. In order to ensure this, we then require that the velocity difference across a smoothing kernel is subsonic, i.e.  $h\Omega < c_s$ , where  $h$  is the smoothing length. This in turn requires that the smoothing length is smaller than the disc thickness  $H = c_s/\Omega$ . We have indeed checked that, even at the lower resolution of 250,000 particles, the average smoothing length is a fraction  $\approx 0.4$  of the disc thickness.

## 3 THE REFERENCE RUN

In this section we describe the results of our reference simulation, called S1, for which the main parameters are listed in the first line in Table 1. Fig. 1 shows images of the disc structure at different times during the evolution, where  $t = 0$  indicates the time at which the perturber reaches pericenter. The colour scale indicates the logarithm of disc surface density between  $1 \text{ g/cm}^2$  and  $10^4 \text{ g/cm}^2$ . The linear size of the images is 160 AU and the images are centered on the instantaneous position of the primary. The two stars are visible as white dots in this image. The perturbing star is initially in the top right hand corner of panel a. It can be seen that the disc starts off in a marginally stable state and displays a clearly visible spiral structure at  $t \simeq -90.7$  years (panel a). The disc orbits in an anti-clockwise motion. At  $t \simeq -22.3$  (panel b), the perturber begins to interact with the disc. At  $t = 0$  (panel c), the perturber reaches the pericentre. After pericenter passage, the disc structure is significantly perturbed, as shown at  $t \simeq 19.1$  years (panel d). At  $t \simeq 81.2$  years (panel e), there is barely any evidence of the pre-encounter spiral structure and the only visible structure is a pronounced tidal tail. The perturber has also carried away roughly 4% of the primary disc mass, most of it being accreted on the perturber and the remainder forming a small circum-secondary disc, as well as causing some gas ( $\approx 6\%$  of the disc mass) to be scattered away from both stars. At  $t \simeq 302.4$  years (panel f), the spiral structure is completely gone leaving a highly stable larger disc in which fragmentation has been prevented.

Figure 2 shows the radial profile of  $Q$  for the reference case for three different times: the start (solid) and end (dashed) of the simulation, and the time when the perturber reaches the pericentre (dotted). It can be seen that when the perturber reaches the pericentre it has stabilized roughly the whole outer disc. By the end of the simulation, the disc has become stable at all radii. Figure 3 shows the corresponding

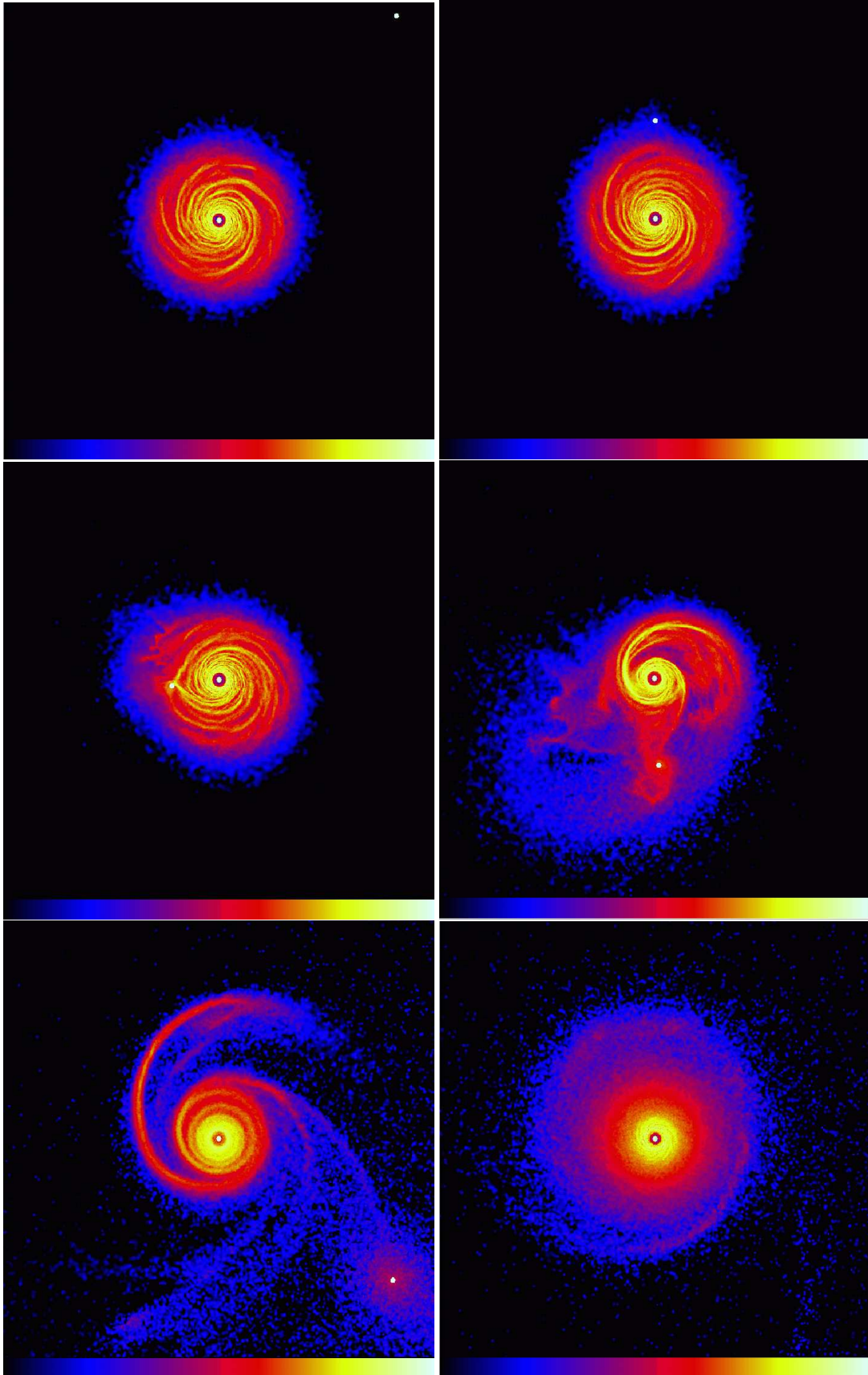


**Figure 1.** Images of the reference simulation at (from top left to bottom right) (a)  $t \simeq -90.7$  yrs (b)  $t \simeq -22.3$  yrs (c)  $t = 0$  yrs (d)  $t \simeq 19.1$  yrs (e)  $t \simeq 81.2$  yrs (f)  $t \simeq 302.4$  yrs

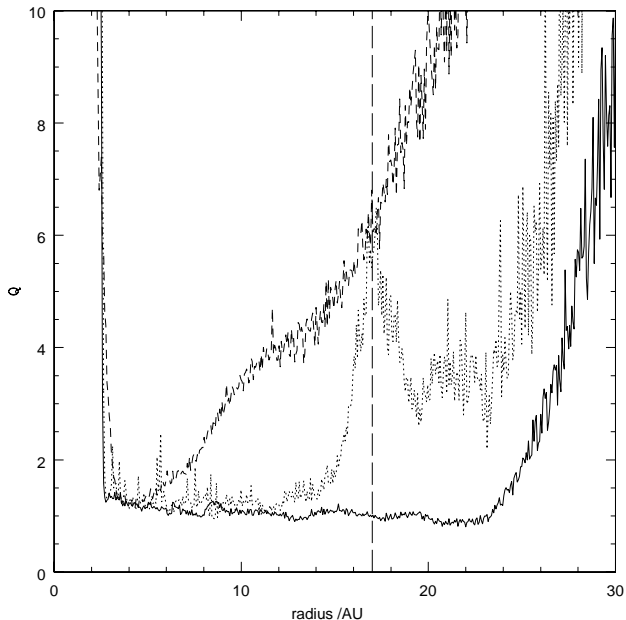


**Figure 2.** Radial profile of  $Q$  at  $t \simeq -90.7$  yrs (solid line),  $t \simeq 0$  yrs (dotted line) and  $t = 302.4$  yrs (dashed line). The vertical dashed line shows the pericentre distance.

plots for the surface density,  $\Sigma$ . There is not much evolution in the surface density before the perturber reaches the pericenter. However, it can be seen that  $\Sigma$  has become significantly steeper at the end of the simulation, suggesting an increase in the accretion rate.

A more detailed view of the effects of the interaction on the disc structure can be obtained from Fig. 4 (solid line), where we plot the evolution of the sound speed and  $Q$  at a radius  $R_r = 8.5$  AU, i.e. halfway between the pericenter and the primary star; the moment at which the perturber reaches pericenter is marked with a dashed line. Several things can be noted from these plots. First of all, the interaction produces a strong increase in sound speed, with the local temperature increasing from about 10 K to more than 100 K within a few decades of pericentre. Thereafter the sound speed declines on the local thermal timescale. The right hand panel shows that  $Q$  tracks the sound speed almost exactly, which is consistent with the fact that changes in  $\Sigma$  at this radius are minor (a few tens of per cent at most). Evidently, the interaction has increased the specific entropy of the material, which must have been mediated by shock heating. Clearly, the net effect of the interaction is to increase  $Q$  and thus to stabilise the disc.

## 4 EXPLORING THE PARAMETER SPACE

### 4.1 Changing the direction of the perturber's orbit

Figure 4 shows a comparison of sound speed and  $Q$  at  $R = 8.5$  AU for the prograde, retrograde and non-coplanar cases (simulations, S1, S3, and S4 respectively). The non-coplanar orbit is set up in such a way so that it impacts the disc at  $90^\circ$ . It can be seen that the largest effect on the

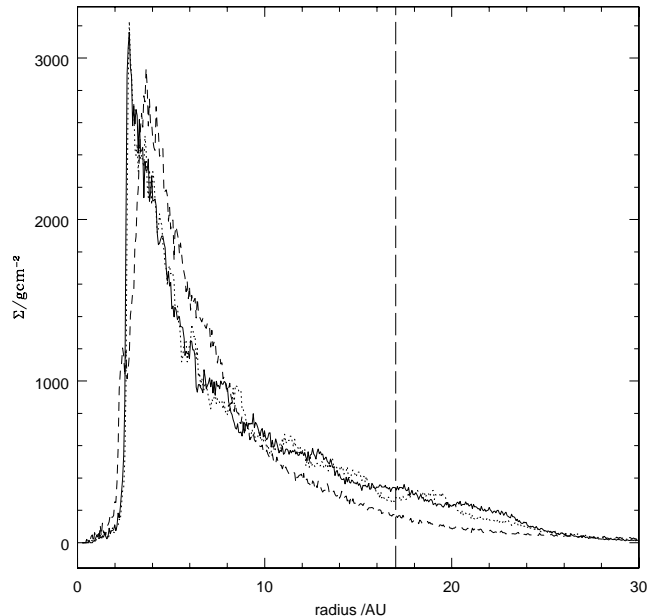


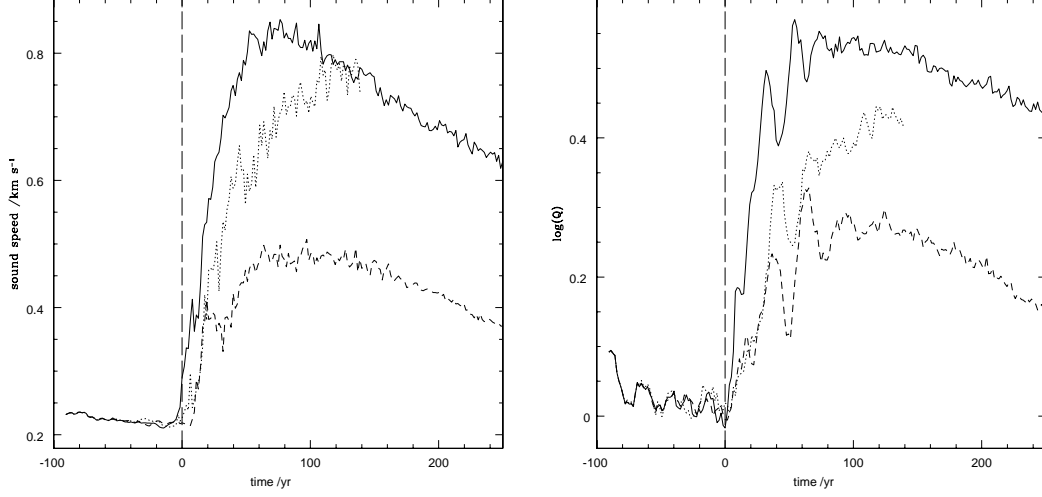
**Figure 3.** Radial profile of  $\Sigma$  at  $t \simeq -90.7$  yrs (solid line),  $t \simeq 0$  yrs (dotted line) and  $t = 302.4$  yrs (dashed line). The vertical dashed line shows the pericentre distance.

disc structure is obtained with a prograde passage, while the retrograde and especially the ‘head on’ encounter have a substantially reduced effect. The fact that the ‘head on’ encounter has a smaller effect can be easily understood since the timescale over which the perturber interacts with the disc is significantly reduced (a similar effect occurs also in the case of a hyperbolic encounter, see below). The comparison between the two coplanar encounters (prograde and retrograde) is in agreement with the results of Hall et al. (1996), who have shown that retrograde encounters induce a smaller amount of angular momentum transfer between the perturber and the disc. We also note that the timescale on which the temperature reaches its peak is roughly double that for the prograde encounter.

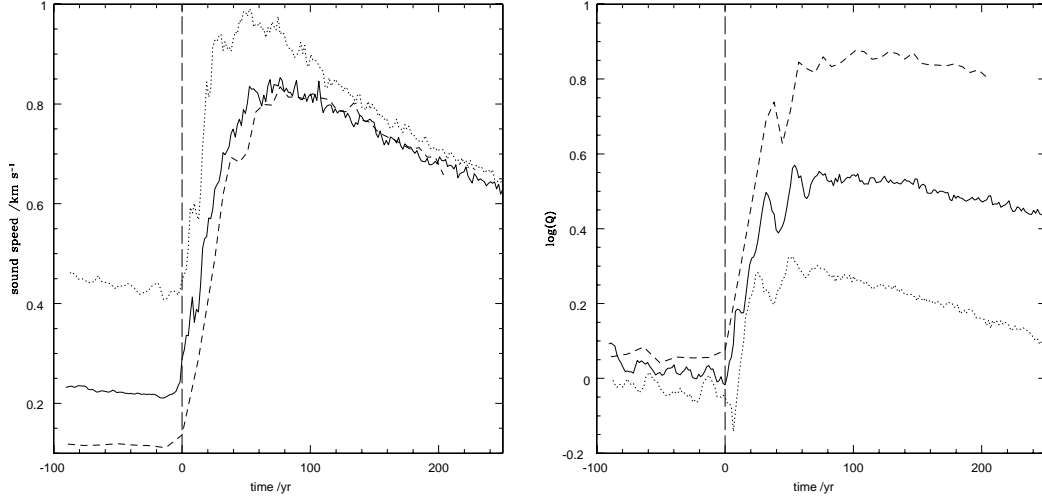
### 4.2 Changing the disc mass

Figure 5 compares the results of simulations S1, S6 and S7, in which we change the disc mass. The sound speed profiles show something interesting: even though the temperature of the higher mass disc is overall the largest, its increase with respect to the pre-encounter value is the lowest, while it is the largest for the lighter disc. This also shows up in the plots of  $Q$ , where for the high disc mass case, the increase in  $Q$  after the encounter is smaller than for the lower disc masses.

Mayer et al. (2005), in their analysis of gravitational instability in binary systems suggested that a lighter disc is more likely to fragment when perturbed by a binary companion as the heating caused by shocks is not enough to balance the large increase in density, thus resulting in a less stable disc. However, the present simulations show that a lower disc mass is stabilized more efficiently than a heavier disc. It appears that the smaller fractional temperature increase



**Figure 4.** Azimuthal averages at  $R = 8.5\text{AU}$  of sound speed (left) and  $\log(Q)$  (right) as a function of time for the simulations involving prograde (solid line), retrograde (dotted line) and non-coplanar (dashed line) orbits.



**Figure 5.** Azimuthal averages at  $R = 8.5\text{AU}$  of sound speed (left) and  $\log(Q)$  (right) as a function of time for simulations S1 (solid line;  $M_{\text{disc}} = 0.1M_{\odot}$ ), S7 (dashed line;  $M_{\text{disc}} = 0.05M_{\odot}$ ) and S6 (dotted line;  $M_{\text{disc}} = 0.2M_{\odot}$ ).

for a high disc mass, with comparable effect on  $\Sigma$ , makes a higher disc mass relatively more susceptible to fragmentation. Nevertheless, we emphasise that for *all* disc masses studied,  $Q$  increases during the encounter, i.e. the effect of the encounter is one of stabilisation.

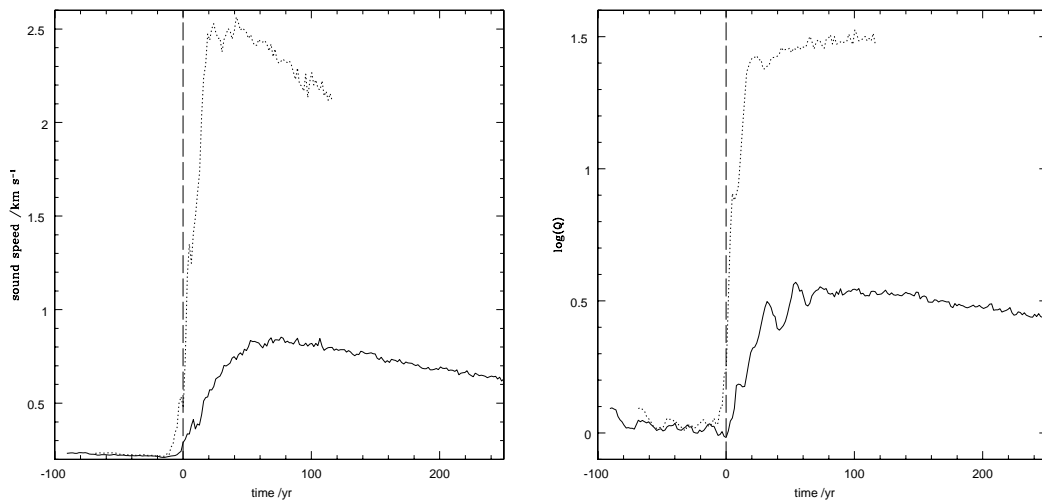
#### 4.3 Changing the perturber's mass

Figure 6 compares the Reference simulation with the simulation with a perturbing star that is ten times heavier (simulations S1 and S2). As expected, increasing the mass of the perturber has a much larger effect on  $Q$ , and sound speed, consistent with more vigorous shock heating. We note that  $Q$  does not in this case just track the evolution of the sound speed, implying that the effect of the higher mass is to decrease the local column density by a factor of a few. This

is indeed confirmed in Fig. 7, that shows the time evolution of the disc surface density for the reference case (solid line) and for simulation S2 (dotted line). While in the reference case after the encounter the surface density is roughly the same as the pre-encounter value, in the high perturber mass case, it is decreased by roughly a factor 3.

#### 4.4 A hyperbolic encounter

In Fig. 8 we show the results of a hyperbolic encounter (simulation S5). In general, the effect is similar to the parabolic one, but smaller in amplitude. This is in general consistent with the fact that the interaction occurs on a much faster timescale for a hyperbolic encounter and is therefore less effective in perturbing the disc structure.



**Figure 6.** Azimuthal averages at  $R = 8.5\text{AU}$  of sound speed (left) and  $\log(Q)$  (right) as a function of time for simulations S1 (solid line;  $M_{\text{pert}} = 0.1M_{\odot}$ ) and S2 (dotted line;  $M_{\text{pert}} = M_{\odot}$ ).

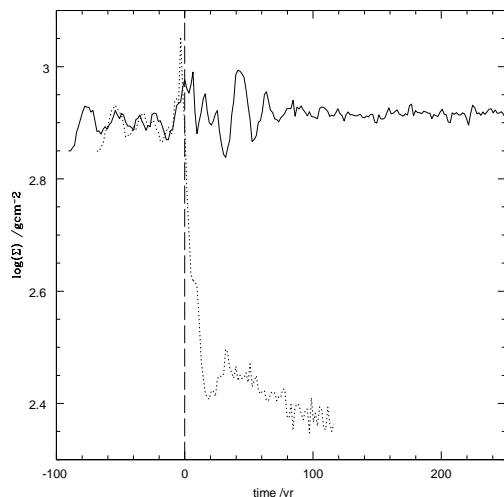


**Figure 7.** Azimuthal averages at  $R = 8.5\text{AU}$  of surface density  $\Sigma$  as a function of time for simulations S1 (solid line) and S2 (dotted line; high perturber mass).

#### 4.5 Changing the pericenter distance

Figure 9 shows that overall, encounters with larger pericenter distances have a much smaller effect on the temperature and  $Q$ . There is slight increase in temperature for the case where  $R_{\text{peri}} = 30$ , whereas for the  $R_{\text{peri}} = 40$  case also the temperature is barely modified.

#### 4.6 A convergence test

Finally, in Fig. 10 we show the results of our convergence test. We have re-run simulation S1 at a higher resolution, by doubling the number of SPH particles used. Figure 10 clearly shows that there is little effect on the temperature and the Toomre parameter when the number of particles is increased to 500,000. Therefore, we can conclude that the

resolution of the reference simulation is adequate and does not affect the outcome of the results.

## 5 DISCUSSION AND CONCLUSIONS

In this paper, we have analysed the effects of an encounter with a discless companion on the structure and evolution of a protostellar disc. We have improved on previous analyses by considering in more detail the energy balance for the gas, thus going beyond the approximation of isothermal evolution used in the past. This turns out to be very important, because the outcome of the encounter is strongly dependent on the tidal heating induced in the disc. Indeed, probably the main result of the present paper is the demonstration that an encounter with a companion inhibits rather than promotes fragmentation of a gravitationally unstable disc. This is in marked contrast with previous results (Boffin et al. 1998), who instead have shown effective fragmentation following an encounter. The main difference between our simulations and those of Boffin et al. (1998) is that while Boffin et al. (1998) consider much larger discs, for which the isothermal approximation is probably adequate, we instead follow the heating and cooling processes in the disc and therefore allow the growth of gravitational instabilities to feed back upon the thermodynamic state of the disc. We include heating from  $p\text{d}V$  work and shocks and cool the disc down with a cooling rate that is sufficiently small that the disc would not fragment in isolation.

We thus conclude that the main parameter that determines the fragmentation of discs is the cooling rate, regardless of the way in which the disc is driven to instability (either through cooling, as in the simulations of Gammie 2001; Mayer et al. 2002; Rice et al. 2003, or by a dynamical interaction, as simulated here). *A disc that does not fragment in isolation, cannot be driven to fragmentation through an interaction with a companion.* Indeed, if anything, tidal heating could prevent fragmentation even in cases where the disc would otherwise fragment, as shown by Mayer et al. (2004)

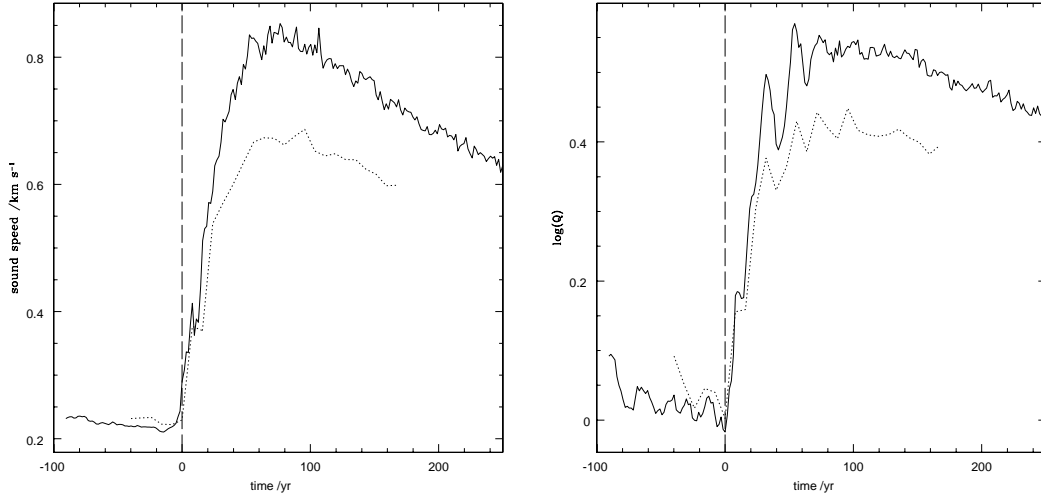


**Figure 8.** Azimuthal averages at  $R = 8.5\text{AU}$  of sound speed (left) and  $\log(Q)$  (right) as a function of time for simulations S1 (solid line; parabolic encounter) and S5 (dotted line; hyperbolic encounter).

(and previously, but in two dimensions, by Nelson 2000), in the context of discs in a binary system. Boss (2006), on the other hand, has shown that in binary systems, disc fragmentation is indeed possible if the cooling timescale is sufficiently small (estimated to be about 1 – 2 orbital timescales by Boss 2006). We note however, that the discs modelled by Boss (2006) were also shown to fragment even in the absence of binary companions. Here again, it would therefore appear, that the cooling timescale is the main determinant of whether discs fragment or not and that the role of companions in either promoting or suppressing fragmentation is rather minor.

Our simulations adopt a simplified prescription for the cooling. In reality, the cooling timescale is going to depend on disc properties, such as density and opacity. In order to determine the stability of discs against fragmentation it is therefore needed to carefully evaluate the actual cooling rate. In the context considered here, it is then interesting to note that Whitworth et al. (2006) have considered this issue analytically and have shown that, with realistic opacity laws, the effect of an encounter is to reduce the cooling rate, further reinforcing the conclusions obtained in our work.

The simulations presented here involve an encounter between a protostellar disc and a disc-less perturber. Our results are therefore directly comparable to those of Boffin et al. (1998). It is however also interesting to consider the more complex behaviour and the much larger parameter space involved in disc-disc interactions, as considered by Watkins et al. (1998a,b). We postpone this investigation to future analyses.

## ACKNOWLEDGEMENTS

The simulations presented in this work have been performed at the UK Astrophysical Fluid Facility (UKAFF).

## REFERENCES

- Bate M. R., Bonnell I. A., Bromm V., 2003, MNRAS, 339, 577
- Bate M. R., Burkert A., 1997, MNRAS, 288, 1060
- Benz W., 1990, in Buchler J., ed., *The Numerical Modeling of Nonlinear Stellar Pulsations* Kluwer, Dordrecht
- Boffin H. M. J., Watkins S. J., Bhattal A. S., Francis N., Whitworth A. P., 1998, MNRAS, 300, 1189
- Bonnell I., Bastien P., 1992, ApJ, 401, 31
- Boss A. P., 2006, ApJ, 641, 1148
- Clarke C. J., Pringle J. E., 1993, MNRAS, 261, 190
- Gammie C. F., 2001, ApJ, 553, 174
- Goodwin S. P., Kroupa P., Goodman A., Burkert A., 2006, ArXiv Astrophysics e-prints
- Hall S. M., Clarke C. J., Pringle J. E., 1996, MNRAS, 278, 303
- Lodato G., Rice W. K. M., 2004, MNRAS, 351, 630
- Lodato G., Rice W. K. M., 2005, MNRAS, 358, 1489
- Mayer L., et al., 2002, Science, 298, 1756
- Mayer L., Quinn T., Wadsley J., Stadel J., 2004, ApJ, 609, 1045
- Mayer L., Wadsley J., Quinn T., Stadel J., 2005, MNRAS, 363, 641
- Mejia A. C., Durisen R. H., Pickett M. K., Cai K., 2005, ApJ, 619, 1098
- Monaghan J. J., 1992, ARA&A, 30, 543
- Nelson A. F., 2000, ApJ, 537, L65
- Rice W. K. M., Armitage P. J., Bate M. R., Bonnell I. A., Jeffers S. V., Vine S. G., 2003, MNRAS, 346, L36
- Rice W. K. M., Lodato G., Armitage P. J., 2005, MNRAS, 364, L56
- Scally A., Clarke C., 2001, MNRAS, 325, 449
- Watkins S. J., Bhattal A. S., Boffin H. M. J., Francis N., Whitworth A. P., 1998a, MNRAS, 300, 1205
- Watkins S. J., Bhattal A. S., Boffin H. M. J., Francis N., Whitworth A. P., 1998b, MNRAS, 300, 1214
- Whitworth A., Bate M. R., Nordlund A., Reipurth B., Zinnecker H., 2006, ArXiv Astrophysics e-prints



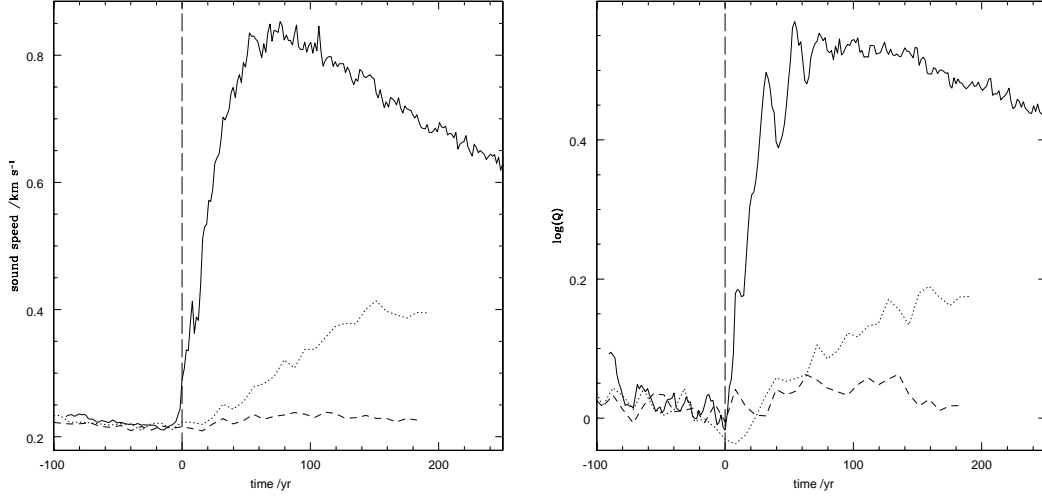


**Figure 9.** Azimuthal averages at  $R = 8.5\text{AU}$  of sound speed (left) and  $\log(Q)$  (right) as a function of time for simulations S1 (solid line;  $R_{\text{peri}} = 17\text{AU}$ ), S8 (dotted line;  $R_{\text{peri}} = 30\text{AU}$ ) and S9 (dashed line;  $R_{\text{peri}} = 40\text{AU}$ ).

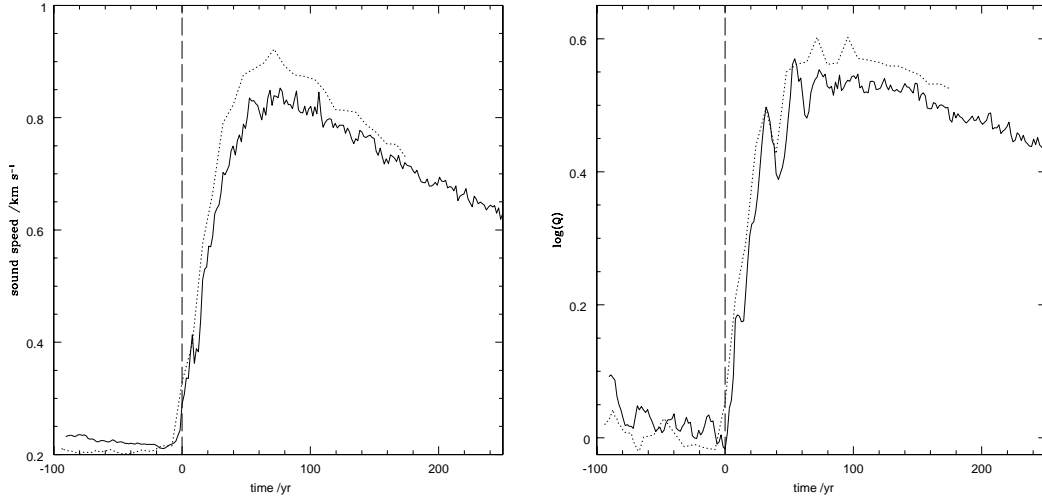


**Figure 10.** Azimuthal averages at  $R = 8.5\text{AU}$  of sound speed (left) and  $\log(Q)$  (right) as a function of time for simulations S1 (solid line; 250,000 particles) and H1 (dotted line; 500,000 particles).